Published in final edited form as:
*Cell*. 2008 June 27; 133(7): 1202–1213.

# The structural basis for activation of the Rab Ypt1p by the TRAPP membrane tethering complexes

**Yiying Cai**[1,4], **Harvey F. Chin**[2], **Darina Lazarova**[1,4], **Shekar Menon**[1,4], **Chunmei Fu**[1], **Huaqing Cai**[1,4], **Anthony Sclafani**[1,4], **David W. Rodgers**[3], **Enrique M. De La Cruz**[2], **Susan Ferro-Novick**[1,4,*], and **Karin M. Reinisch**[1,*]

1 *Department of Cell Biology, Yale University School of Medicine, 333 Cedar Street, New Haven, Connecticut 06520*

2 *Department of Molecular Biophysics and Biochemistry, Yale University, 260 Whitney Avenue, New Haven, Connecticut 06520*

3 *Department of Molecular and Cellular Biochemistry, University of Kentucky, College of Medicine, 741 S. Limestone Boulevard, Lexington, KY 40536*

4 *Howard Hughes Medical Institute*

## Summary

The multimeric membrane tethering complexes TRAPPI and TRAPPII share seven subunits, of which four (Bet3p, Bet5p, Trs23p, and Trs31p) are minimally needed to activate the Rab GTPase Ypt1p in an event preceding membrane fusion. Here we present the structure of a heteropentameric TRAPPI assembly complexed with Ypt1p. We propose that TRAPPI facilitates nucleotide exchange primarily by stabilizing the nucleotide binding pocket of Ypt1p in an open, solvent-accessible form. Bet3p, Bet5p, and Trs23p interact with Ypt1p directly to stabilize this form, while the C terminus of Bet3p invades the pocket to participate in its remodeling. The Trs31p subunit does not interact directly with the GTPase but allosterically regulates the TRAPPI interface with Ypt1p. Our findings imply that TRAPPII activates Ypt1p by an identical mechanism. This first view of a multimeric membrane tethering assembly complexed with a Rab provides a framework for understanding events preceding membrane fusion at the molecular level.

## Introduction

In eukaryotic cells, vesicles transport materials between membrane bound compartments. After a vesicle buds from a donor membrane, it travels through the cytoplasm to its target membrane, where it fuses to deliver its cargo. This membrane fusion event is mediated by SNAREs, a family of membrane proteins located on the vesicle and target membranes (Jahn & Scheller, 2006). Vesicle transport, however, also requires the interplay of a large number of peripheral membrane proteins that act upstream of the SNAREs. These include coat proteins that are needed for cargo selection and vesicle budding, tethering proteins, and small GTPases of the Rab family involved in regulation. Tethers are either long coiled-coil proteins or large

*To whom correspondence should be addressed (e-mail to susan.ferronovick@yale.edu or karin.reinisch@yale.edu).

**Accession Number**
The coordinates have been deposited in the Protein Data Bank with the accession code 3CUE.

multimeric complexes that mediate the initial interaction of the vesicle and its target membrane (reviewed in Cai *et al*., 2007a).

TRAPPI is one of the best characterized multiprotein tethering complexes. First described in the yeast *S. cerevisiae* (Sacher *et al.*, 1998), TRAPPI subunits are present in all eukaryotes (Koumandou *et al.*, 2007). In yeast, TRAPPI mediates the tethering of endoplasmic reticulum (ER)-derived COPII coated vesicles at the cis-Golgi (Sacher *et al*., 1998). Tethering involves interactions between the TRAPPI subunit Bet3p and Sec23p (Cai et al, 2007b), a component of the COPII coat adapter complex (Kuehn *et al.*, 1998). This interaction targets a COPII vesicle to the Golgi (Cai *et al*., 2007b). Critically, TRAPPI also functions as a guanine nucleotide exchange factor (GEF) for the Rab GTPase Ypt1p (Sacher *et al.*, 2001), facilitating the conversion of the inactive GDP-bound form of Ypt1p to the active GTP-bound form. Membrane fusion proceeds only once Ypt1p is activated by TRAPPI (Cai *et al.*, 2007a). TRAPPI shares multiple subunits with the TRAPPII complex, which mediates trafficking events within the Golgi and from the early endosome to the late Golgi (Cai *et al*., 2005).

The TRAPPI complex comprises seven small subunits (2 copies of Bet3p and one copy each of Bet5p, Trs20p, Trs23p, Trs31p, and Trs33p), which range in size from 18–33 kDa, as well as a larger 80 kDa protein Trs85p (Sacher *et al.*, 1998, Sacher *et al*., 2000). Except for Trs33p and Trs85p, all of the TRAPPI subunits are required for cell viability (Sacher *et al.*, 1998, Sacher *et al.*, 2000). Unusually, TRAPPI GEF activity does not reside on any one subunit (Kim *et al*., 2006; Cai *et al*., 2007b) but requires a minimal complex of Bet3p, Bet5p, Trs23p, and Trs31p (Kim *et al.*, 2006). The requirement of complex assembly as a prerequisite for GEF activity may allow for additional regulation of vesicle transport.

To understand how TRAPPI subunits cooperate in activating Ypt1p, we have determined the crystal structure of a TRAPPI subassembly in complex with Ypt1p at a resolution of 3.7 Å. The structure offers the first snapshot of the interactions between a multimeric membrane tethering complex and a Rab GTPase. The TRAPPI subcomplex studied contains the minimum number of subunits (2 copies of Bet3p and one each of Bet5p, Trs23p, and Trs31p) needed to activate Ypt1p (Kim *et al*., 2006), and in the structure, this assembly stabilizes the GTPase in its intermediate, nucleotide-free form. A comparison of nucleotide-free Ypt1p with existing nucleotide bound structures of the enzyme (PDB ID 1YZN; Eathiraj *et al.*, 2005) or its mammalian homolog Rab1a (PDB ID 2FOL) allows us to propose a mechanism for guanine nucleotide exchange in which each subunit in the TRAPPI subassembly contributes to the activity of this multimeric GEF.

## Results and Discussion

### Overview of the TRAPPI subcomplex

The crystal structure of a TRAPPI subassembly (Figure 1A–C) consisting of one copy each of Bet5p, Trs23p, and Trs31p, and two copies of Bet3p (named Bet3p-A and Bet3p-B) was determined in complex with a C-terminally truncated Ypt1p (residues 1–180). Data collection and refinement statistics are shown in Table S1. The 26-residue Ypt1p C terminus that was truncated is not required for activation of nucleotide exchange by TRAPPI (data not shown).

The TRAPPI subassembly is about 135 Å long and 30–75 Å in diameter (Figure 1A). One of its surfaces is largely acidic, whereas the other has both basic and acidic regions (Figure 1B). Bet3p-A, Bet5p, Trs23p, and Bet3p-B are arranged end-to-end along the length of the complex (Figure 1A, C). Bet3p-A/Bet5p and Bet3p-B/Trs23p are related by a 2-fold rotation around an axis centered at the Bet5p/Trs23p interface. Trs31p binds at one end of the otherwise cylindrical complex, interacting with both Trs23p and Bet3p-B.

The yeast small TRAPPI subunits in the crystal structure have mixed alpha/beta topologies (Figure 1C) similar to those previously described for their vertebrate homologs (Kim *et al.*, 2006, Kim *et al*., 2005b, Turnbull *et al.*, 2005). Despite limited sequence homology, Bet5p and Trs23p (20% sequence identity) share a common fold, as do Bet3p and Trs31p (15% sequence identity). The yeast Trs23p protein does not have the PDZ-like domain described for the mammalian protein, and insertions in the yeast proteins with respect to the mammalian sequences are for the most part disordered in the crystal structure. These insertions include residues 76–103 and 148–168 in Trs23p and residues 1–54 and 104–164 in Trs31p. Bet3p has an additional N-terminal alpha helix, which plays a role in subunit interactions. Importantly, the C-terminal residues of Bet3p, disordered in all existing structures of the mammalian homolog (Kim *et al.*, 2005a, Kim *et al*., 2005b; Turnbull *et al*., 2005; Kummel *et al.*, 2006b, and in TRAPP subcomplexes as in Kim *et al.*, 2006), are ordered in the Ypt1p/TRAPPI complex, where they are involved in intermolecular contacts with Ypt1p.

A deep channel lined by hydrophobic residues traverses each of the Bet3p subunits. Bet3p is palmitoylated via a thioester linkage to a conserved cysteine (C80) (Turnbull *et al.*, 2005). We have modeled a palmitoylate group into the channel of Bet3p-A, where we find density continuous with Cys80 in averaged composite omit maps (Figure S1). The bound fatty acid is less well defined in Bet3p-B, though there is electron density deep in the channel corresponding to 8–9 methylene groups of the hydrocarbon tail. The palmitoyl group has been shown to contribute to the stability of Bet3p (Kummel *et al.*, 2006). Mutational analysis suggests, however, that neither the palmitoyl group (Kim *et al*., 2005a, Turnbull *et al.*, 2005) nor the hydrophobic channel (Figure S2) are essential for TRAPP function.

## Ypt1p interactions with TRAPPI

The Ypt1p binding site is on the acidic surface of the TRAPPI subassembly. The interface is formed primarily by the Trs23p subunit with smaller contributions from the two copies of Bet3p and Bet5p (see Figure 1A, B). The total accessible surface buried in the interface between Ypt1p and TRAPPI is 2990 $Å^2$. Accessible surfaces buried in the interfaces with Trs23p, Bet3p-A and B, and Bet5p measure ~1870, ~650, ~250 and ~250 $Å^2$, respectively. There is no direct interaction between Ypt1p and Trs31p. TRAPPI interacts (Figure 2) primarily with residues in the central beta sheet of Ypt1p (in strands S1, S2, and S3), the switch I and II regions (residues 31–45 and 64–78), and the phosphate binding loop, or P-loop (residues 15–23). Switches I and II are those regions in the nucleotide binding pocket that adopt different conformations in the active and inactive forms of Ypt1p, and the P-loop is important in binding the β- and γ-phosphates of nucleotides.

Structures are available for Ypt1p in complex with the non-hydrolysable GTP analog guanosine-5′ (β,γ) imidotriphosphate (GppNHP) (PDB ID 1YZN; Eathiraj *et al.*, 2005) and its mammalian homolog Rab1a, bound to GDP (PDB ID 2FOL). Rab1a is nearly identical to Ypt1p over most of its sequence. In the Ypt1p/TRAPPI complex, the Ypt1p N terminus (residues 4–10, where 7–10 are in beta-strand S1) contacts Trs23p and has shifted with respect to nucleotide bound forms (Figure 2, 3). Small shifts in adjacent structural elements, the loop between strands S2 and S3 (residues 53–54) as well as the C terminus (residues 150–174, including H5), accompany the change in the N terminus.

The most dramatic changes in Ypt1p, however, are in the nucleotide binding pocket. Residues 150–155 in a loop at the Ypt1p C-terminus form part of this pocket. In the Ypt1p/TRAPPI complex, they are shifted into the pocket close to the position occupied by the guanosine base in nucleotide bound structures. The Ala152 Cβ would be within 2 Å of atoms in the guanosine base, in a position incompatible with nucleotide binding.

The nucleotide binding pocket is further perturbed by the insertion of the Bet3p-A C terminus, which would clash sterically (particularly at residues 189–193) with switch I as oriented in nucleotide bound forms of Ypt1p/Rab1a (Figure 3A, B). The switch I region (residues 27–45) of Ypt1p is rearranged relative to its nucleotide bound conformations (Figure 3A, B), opening up the nucleotide binding pocket. In their new conformation, switch I residues 37–45 contact the Bet3-A C-terminus as well as residues in helix H1 of Bet5p and helix H1 of Trs23p (Figure 2). Residues 32–36 in the middle of switch I are not well ordered in the complex structure. In the nucleotide bound form, the highly conserved Tyr33 from this sequence contacts the guanine base via an edge-to-face aromatic interaction (Eathiraj *et al.*, 2005; PDB IDs 1YZN, 2FOL). Mutating this residue to alanine (Y33A) accelerates GDP release by ~10-fold (Figure 3C) while not affecting nucleotide uptake (Figure 3D), thereby lowering Ypt1p affinity for GDP by an order of magnitude. Thus, the perturbation of Tyr33 during switch I reorganization would similarly be expected to weaken the affinity for GDP in the TRAPPI-bound form of Ypt1p and to accelerate GDP release by roughly an order of magnitude.

The switch II region of the nucleotide binding pocket also alters its conformation in the Ypt1p/TRAPPI complex. Switch II residues are disordered in the Rab1a/GDP structure (PDB ID 2FOL), and their conformation differs in the active and the TRAPPI-bound forms of Ypt1p (Figure 3A, B). In the Ypt1p/TRAPPI complex, switch II is folded against a surface formed by helices H1 of Trs23p, H1 of Bet5p, and residues near the C terminus of Bet3p-B of TRAPPI. This interaction drives the formation of a helix (H2; Figures 2 and 3A, B) and moves switch II residues out of the nucleotide binding pocket as compared with their position in activated Ypt1p.We will discuss the implications of switch II folding below.

The conformation of the P-loop in TRAPPI-bound Ypt1p is similar to that in nucleotide-bound forms of Ypt1p and Rab1a. In the Ypt1p/TRAPPI complex, the loop is stabilized in part by a hydrogen bonding interaction between the P-loop residue Lys21 and Glu192 in the Bet3p-A C-terminus (Figure 3A, B). As modeled, this glutamate side chain (including Cβ, Cγ, as well as the carboxylate group) would be within 1.6 Å of the nucleotide phosphates in the nucleotide bound forms of Ypt1/Rab1a, in a position incompatible with nucleotide binding. The sequence identity of residue 192 is not critical for nucleotide exchange, however, as the E192A/D193A double mutation in the Bet3p C terminus has only a small effect on GEF efficiency (Table 1, Figure 4A).

## TRAPPI mutants with impaired GEF activity

Our structural studies suggest that the Bet3p-A C terminus, which is inserted into the Ypt1p nucleotide binding site, may play an important role in guanine nucleotide exchange. The C terminus may be important for initiating the conformational changes in switch I that help to catalyze nucleotide exchange. Additionally, contacts with the Bet3p C terminus seen in the structure (Figure 2) may be important for stabilizing switch I in its new conformation. To assess the importance of the Bet3p C-terminus for exchange, we prepared TRAPPI subassemblies that incorporate C-terminally truncated versions of Bet3p. Constructs of Bet3p that contained 185, 188, or 191 residues of the 193 amino acid sequence catalyzed nucleotide exchange at least 150-fold less efficiently than the TRAPPI complex with full-length Bet3p (Table 1, Figure 4A,B), consistent with a critical role for the entire Bet3p C terminus in the exchange mechanism.

Mutations in other TRAPPI surfaces at the Ypt1p interface would also be expected to affect Ypt1p recognition and possibly nucleotide exchange. Indeed, we were able to entirely, or almost entirely, eliminate TRAPPI GEF activity by mutating surface patches on any one of three different subunits: Bet3p, Bet5p, or Trs23p (Table 1, Figures 4B,D). We found that mutations in the Trs23p surface that interacts with strand S1 in the Ypt1p N terminus (S12K/G14M/L34K and M200A/P201W/R203S) abrogate GEF activity entirely (Table 1, Figures

4B). Similarly, mutations designed to interfere with a switch I interaction, a double mutation in Bet5p (G46W/S50K) or a point mutation in Trs23p (S38R), completely inactivated TRAPPI (Table 1, Figures 4B). Finally, a quadruple mutation in Trs23p (H41A/G42M/A45W/I46R) at the switch II binding surface of TRAPPI, reduced the catalytic efficiency to residual levels (Table 1, Figure 4B).

In addition to assessing the consequences of each of these mutations *in vitro*, we also examined their effect on viability in yeast. Two different methods were used to construct the mutants. The C-terminal truncations of Bet3p were constructed using the method of Longtine *et al.* (1998). For the other mutations, a mutant copy of each gene was constructed by site directed mutagenesis on a *CEN* plasmid (*LEU2*) and then transformed into a strain in which the sole copy of the wild type gene was on a *CEN* balancing plasmid (*URA3*). The balancing plasmid with the wild type gene was subsequently lost on a 5-FOA (5-fluoroorotic acid) plate, allowing us to evaluate the effect of the mutation on growth. We found that TRAPP mutants lacking all GEF activity *in vitro* were inviable (Table 1, Figure 4C). Mutants with residual *in vitro* activity grew as well as wild type at 25°C or 37 °C, however, and did not display defects in invertase secretion (Table 1, Figures 4C, S3). A likely explanation for this apparent anomaly is that TRAPPI may act more effectively in the cell than *in vitro*. Soluble TRAPPI and Ypt1p were used *in vitro*, whereas in cells Ypt1p is anchored to a membrane via its prenylated C terminus and exchange occurs at the membrane. Thus, the effect of certain mutations may be less pronounced *in vivo* than *in vitro*.

## Mechanism for Ypt1p activation

Biochemical solution studies of nucleotide binding and exchange reveal the kinetic basis of Ypt1p activation by TRAPPI. TRAPPI accelerates the dissociation of Ypt1p-bound GDP ($k_{-GDP}$) >400-fold (Table 1, *k*Figure 4A). The initial velocities of [TRAPPI]-dependent nucleotide exchange (Table 1, Figure 4A) yield apparent second order rate constants for TRAPPI activation of nucleotide exchange from Ypt1p (equivalent to the enzymatic $_{cat}/K_m$) and serve as a practical reference with which to assess the catalytic efficiency of a GEF (Itzen *et al*., 2006). The catalytic efficiency of TRAPPI,.016 ± .001 $\mu M^{-1}s^{-1}$, is intermediate between two other characterized Rab GEF's, Vps9 and Sec2p. (Esters *et al*., 2001;Itzen *et al.*, 2007). In addition, TRAPPI accelerates GTP binding to Ypt1p ($k_{+GTP}$) ~30-fold (Figure 4E), more than has been observed for other Rab GEF's (Esters *et al*., 2001;Itzen *et al.*, 2007), but comparable to non-Rab GEF's (Klebe *et al*., 1995). The acceleration of nucleotide dissociation and binding serve as a framework for formulating structure-based models of TRAPPI-mediated nucleotide exchange from Ypt1p.

The structure and kinetic analysis of TRAPPI mutants (Table 1, Figure 4) suggest an important role for the Bet3p-A C terminus in the guanine nucleotide exchange mechanism. In the structure, which represents an intermediate in exchange following release of bound nucleotide, the Bet3p-A C terminus invades the GTPase nucleotide binding pocket. We propose that the Bet3p-A C terminus functions in the remodeling of switch I that promotes the release of bound nucleotide. Conformational changes in switch I open the nucleotide binding pocket and in effect uncage bound nucleotide to facilitate GDP release. Additionally, switch I remodeling removes Tyr33, which stabilizes bound nucleotide (Eathiraj *et al*., 2005), from the binding site. This likely also plays a role in accelerating GDP release. Based on our kinetic analysis of the Ypt1p Y33A mutant, however, we would expect at most a 10-fold increase in GDP release with loss of the Tyr33 contact. The more than 400-fold acceleration in GDP release effected by TRAPPI must also result from other factors, such as the opening of the nucleotide binding pocket discussed above. The Tyr33 perturbation does, however, help to explain the lower affinity of the TRAPPI-bound form of Ypt1p for GDP, which is an order of magnitude weaker than that of Ypt1p (unpublished observation). The shift of the Ypt1p 150's loop (residues 150–

155) into a site close to that normally occupied by the guanosine base, which is induced by interactions with TRAPPI, may also weaken the affinity of Ypt1p for nucleotide. The final step of the nucleotide exchange reaction involves GTP uptake, which is accelerated by TRAPPI (Figure 4E). Holding switch I in an open conformation which makes the pocket more solvent accessible likely accounts at least partly for this acceleration. The folding of switch II, which adopts similar conformations in the Ypt1p/TRAPPI complex and in the GTP-bound form of Ypt1p (Figure 3A,B), would also contribute to faster GTP association with the TRAPPI-bound form of the GTPase. Elements of TRAPP, particularly the Bet3p-A C terminus, occupy a part of the nucleotide binding pocket in the complex with Ypt1p. Any decrease in the rate of GTP binding that results from the need for these elements to exit the binding site must be more than compensated for by the favorable conformations of switches I and II.

All known GEFs reconfigure the nucleotide binding pocket, often opening it by rearranging the switch regions (reviewed in Bos *et al.*, 2007). Many GEFs facilitate this rearrangement by inserting a protein “wedge” into either the magnesium or the nucleotide binding site (Bos *et al.*, 2007). With TRAPPI, the C-terminal end of Bet3p-A may be functionally equivalent to a wedge, though it differs mechanistically in that it is not a rigid structural element and may be poorly ordered in the absence of Ypt1p. TRAPPI is similar to GEFs for Ras and several of the Rab GTPases (Boriack-Sjodin *et al.*, 1998; Delprato & Lambright, 2007; Dong *et al.*, 2007; Sato *et al.*, 2007) in that the guanine nucleotide exchange mechanism involves the displacement of a conserved aromatic residue required for nucleotide stabilization. In Ypt1p this aromatic side chain is Tyr33.

TRAPPI differs most strikingly from other GEFs in that its exchange activity is linked to the assembly of a multimeric subcomplex. Our structure delineates a role for each of the subcomplex proteins in nucleotide exchange. TRAPPI provides a surface against which regions of Ypt1p are reorganized into their nucleotide-free conformation. Most of this surface is formed by the Trs23p subunit, but smaller contributions from Bet3p (A and B) and Bet5p are also important (Figure 2). Indeed, we have shown that mutations in the surfaces of any of the three proteins can interfere with TRAPPI GEF activity (Table 1, Figure 4). Additionally, Bet5p has a major structural role both as a linker between Trs23p and Bet3p-A and in directing the Bet3p-A C-terminal residues toward the Ypt1p nucleotide binding pocket. The C terminus of Bet3p-A, which perturbs the nucleotide binding pocket in the Ypt1p/TRAPP complex, enhances the efficiency of guanosine nucleotide exchange.

Trs31p does not interact with Ypt1p directly, and yet a TRAPPI subcomplex lacking Trs31p does not activate Ypt1p (Kim *et al.*, 2006). Comparison of our structure with those of the vertebrate complexes Trs20/Bet3-B/Trs31 and Trs23/Bet5/Bet3-A/Trs33 (PDB IDs 2J3W, 2J3T; Kim *et al.*, 2006), neither of which has GEF activity (Kim *et al*., 2006; Cai *et al*., 2007b), suggests that Trs31p promotes GEF activity by affecting the conformation of Trs23p at the Ypt1p binding interface. Bet3p-B/Trs31p and Trs23p/Bet5p/Bet3p-A subcomplexes from yeast and vertebrates superimpose well (rmsd values of just 1.8 Å on 317 equivalent Cα positions and 2.4 Å on 414 equivalent Cα positions, respectively). However, the structures differ significantly at the three-way interface between Trs23p, Trs31p, and Bet3p-B (Figure 5). The formation of this TRAPPI interface, which is not present in either of the vertebrate complex structures, causes complementary shifts in elements of Trs31p and Trs23p. In particular, the connecting loop between strand S2 and helix H4 of Trs31p moves toward Trs23p, and helices H2 and H3 of Trs23p with their connecting loop shift by up to 12 Å to accommodate the new position of the Trs31p loop. The shifted connecting loop in Trs23p interacts with Ypt1p (strand S1) in the Ypt1p/TRAPPI complex (see Figure 2), and this interaction is important for GEF activity since mutations in the loop (M200A/P201W/R203S) abolish GEF function (Table 1, Figure 4B). Thus binding of the GTPase may depend on conformational changes resulting from the formation of the Trs23p/Trs31p/Bet3p-B interface.

Alternatively, the formation of the 3 way interface may stabilize conformational changes that only occur upon Ypt1p binding. The importance of the Trs23p/Trs31p/Bet3p-B interface for GEF activity is supported by the finding that a double mutation in Trs23p (T136E/Y183D) at this interface abolishes TRAPPI activation of Ypt1p (Kim *et al*., 2006).

In summary, Bet3p, Bet5p, and Trs23p are essential for Ypt1p binding, with the C-terminus of Bet3p-A playing a critical catalytic role in the exchange mechanism. Bet5p is necessary for the assembly of the GEF core; and Trs31p and likely also Bet3p-B appear to function allosterically by affecting the conformation of Trs23p.

## TRAPPII is also a Ypt1p Exchange Factor

To date, ten different TRAPP subunits have been identified (Sacher *et al*., 2000). TRAPPI and TRAPPII share seven of these subunits, while three subunits (Trs65p, Trs120p, and Trs130p) are unique to the larger TRAPPII complex (Sacher *et al*., 2001). The observation that TRAPPII contains all of the subunits that are essential for Ypt1p activation prompted us to determine if TRAPPII is also a Ypt1p GEF. To isolate fully assembled TRAPPI and TRAPPII complexes, we used a yeast strain in which Protein A tagged Bet3p replaced the endogenous protein. The tag we used has no appreciable effect on the assembly of the TRAPP complexes (Cai *et al*., 2005) or on Ypt1p activation (Wang *et al*., 2000). Lysate prepared from this strain was sieved on a Superdex-200 column to separate TRAPPI and TRAPPII, as described previously (Sacher *et al*., 2001). Fractions containing either complex were then incubated with IgG Sepharose beads and washed. An analysis of the subunits present showed that both Trs33p and Trs130p were on the TRAPPII containing beads, while TRAPPI coated beads contained only Trs33p (data not shown). We found that TRAPPII potently stimulates nucleotide exchange on Ypt1p (Figure 6A). Furthermore, when we normalized guanine nucleotide exchange activity to the amount of Trs33p present in each fraction, TRAPPII and TRAPPI had comparable activity (Figure 6A). As would be expected for a Ypt1p GEF, TRAPPII binds to both nucleotide-bound forms of the GTPase and preferentially to the GDP-bound form (Figure 6B). Our results differ from earlier studies that suggested that TRAPPII is not an exchange factor for Ypt1p (Morozova *et al*., 2006). In that study, TRAPP complexes were isolated from a strain overexpressing GST-tagged Bet5p, and one explanation is that the GST-tag on Bet5p may have interfered with Ypt1p activation.

The same study suggested that the addition of TRAPPII-specific subunits converts TRAPPI into a GEF for Ypt31p and its functionally redundant homolog Ypt32p (Morozova *et al*., 2006; also Jones *et al*., 2000), but we have been unable to repeat these results with our TRAPPII preparations (Figure 6C, D). We have also found that a mixture of TRAPP complexes, isolated using TAP-tagged Trs33p, did not activate Ypt32p efficiently (Wang & Ferro-Novick, 2002). The result that TRAPPII does not stimulate exchange for Ypt31p/Ypt32p efficiently is consistent with a previous report showing that depletion of TRAPPI and TRAPPII from yeast lysates eliminates Ypt1p GEF activity without affecting GEF activity on Ypt32p (Wang & Ferro-Novick, 2002). Also consistent with the finding that TRAPPII is not a GEF for Ypt31p/Ypt32p, we are unable to detect an interaction between TRAPPII and Ypt31p-GDP *in vitro* (data not shown). Thus, we conclude that TRAPPII is an exchange factor for Ypt1p and is unlikely to be the exchange factor for Ypt31p/Ypt32p *in vivo*.

In addition to acting in ER-Golgi traffic, Ypt1p also functions at the late Golgi (Sclafani and Ferro-Novick, unpublished observations; Cai *et al*., 2007a). In this respect it differs from its mammalian homolog Rab1, which only mediates membrane transport between the ER and Golgi (Moyer *et al*., 2000). Our data indicate that TRAPPII is the Ypt1p GEF that functions at the late Golgi. Importantly, the finding that TRAPPII is a Ypt1p GEF implies that the Ypt1p binding site that we identified for TRAPPI remains accessible in TRAPPII. We conclude that TRAPPI and TRAPPII almost certainly activate Ypt1p by an identical mechanism.

### TRAPP tethering

The superposition of the two vertebrate subcomplexes, Trs20/Bet3-B/Trs31 and Bet3-A/Bet5/Bet3-A/Trs23/Trs33 with yeast Bet3p-A/Bet5p/Trs23p/Bet3p-B/Trs31p described here, gives a model of the intact TRAPPI complex (Figure 5A). In the larger assembly, Trs20 interacts with Bet3-B/Trs31 and Trs33 interacts with Bet3-A/Bet5. The model is in agreement with a model proposed on the basis of the vertebrate subcomplexes and a ~30 Å single particle reconstruction of yeast TRAPPI (Kim *et al.*, 2006).

The symmetry of TRAPPI suggests a mechanism by which this complex mediates vesicle tethering. It is known that Bet3p interacts with the Sec23p subunit of the COPII vesicle coat (Cai *et al.*, 2007b). In mammals it has been demonstrated that the TRAPP complex mediates homotypic tethering between two COPII coated vesicles (Yu *et al.*, 2006). We therefore speculate that TRAPP interacts similarly with both vesicles *via* the two copies of Bet3 (see also Cai *et al.*, 2007b) located at either end of the core complex as shown in Figure 5B. Bet3-A and Bet3-B would interact with the COPII subunit Sec23 using the same surfaces because of symmetry present in the TRAPP complex. Equivalent surfaces on Bet3-A and –B are accessible to both vesicles only if TRAPP is oriented as shown, since in any other orientation binding by only one vesicle would block access to both of the equivalent Bet3 surfaces. In yeast, the architecture of the secretory pathway differs, and TRAPPI mediates heterotypic tethering of a COPII vesicle with the Golgi. Thus, in yeast cells TRAPPI must have the ability to bind a Golgi receptor as well as Sec23p, but we speculate that the arrangement of the tethering complex with respect to membranes is similar to that for homotypic fusion. This model is consistent with a scenario in which TRAPPI first tethers the secretory vesicle to the Golgi membrane, and then, with the Ypt1p binding site still accessible, recruits and activates the Rab protein. Our model differs from one previously proposed (Kim *et al.*, 2006), which would predict that in homotypic fusion vesicles would interact with TRAPP in two different ways. (Mutational studies presented in Figure S4 show that data previously cited to support this other model is incorrect.)

Our recent observation that Ypt1p regulates both ER-Golgi transport and traffic between the early endosome and late Golgi (Sclafani and Ferro-Novick, unpublished observation) implies that Ypt1p is activated by one or more GEFs at distinct membrane trafficking events. Accordingly, we have shown that TRAPPI, which functions in ER-Golgi traffic, and TRAPPII, which mediates trafficking events within the Golgi and at the late Golgi (Cai *et al.*, 2005), both activate Ypt1p. Presumably TRAPPI and TRAPPII activate Ypt1p by the same mechanism using subunits shared by both complexes. The TRAPP complexes also function as tethers, however, that tether different membranes. TRAPPI, but not TRAPPII, binds to COPII coated vesicles *in vitro* (Sacher *et al.*, 2001), whereas TRAPPII has been implicated in tethering COPI coated vesicles (Cai et al., 2005). Thus, the addition of TRAPPII-specific subunits (Trs65p, Trs120p, and Trs130p) must convert TRAPPI from a tether that mediates interactions between the COPII coat and early Golgi to one that functions in recognition between the COPI coat and late Golgi. Such a conversion implies that the TRAPPII-specific subunits not only mediate these new interactions but that they also mask binding sites on TRAPPI which would allow for interactions with the COPII coat and early Golgi.

## Concluding Remarks

A formidable obstacle in understanding membrane traffic has been the limited knowledge regarding the interactions between the many proteins that coordinate these events. In this work, we have visualized the five proteins of the GEF core of TRAPP as they cooperate to activate Ypt1p. We propose that interactions with four proteins (Bet3p-A, Bet3p-B, Bet5p, and Trs23) in the complex stabilize Ypt1p in an open conformation facilitating nucleotide exchange. The

Trs31p subunit does not interact with Ypt1p directly, but regulates the conformation of Trs23p at the Ypt1p interaction surface.

## Experimental Procedures

Cloning strategies and protocols used for constructing the *bet3*, *bet5*, and *trs23* mutants are detailed in the Supplemental Methods.

### Overexpression and Purification

We prepared several TRAPPI subcomplexes. We were able to obtain crystals only with a complex containing Bet3p, Bet5p, Trs23p, and Trs31p but not additional TRAPPI subunits (Trs20p and/or Trs33p). We used a larger complex that additionally contained Trs20p for guanosine nucleotide exchange assays. This second complex contains all essential TRAPPI subunits and was reported to be indistinguishable from intact TRAPPI as monitored by GDP release and GTP uptake assays (Kim *et al.*, 2006; Cai *et al.*, 2007b).

For overexpression of TRAPPI subcomplexes, three Duet plasmids harboring genes for *BET3*, *BET5*, *TRS23*, *TRS31* and optionally *TRS20* were co-transformed into *E. coli* BL21 (DE3) cells by electroporation. When the cells reached an $OD_{600}$ of ~0.6–0.8, they were shifted to 25 °C, and protein expression was induced with 0.5 mM IPTG. Cells were harvested 18 hrs after induction. Selenomethionine substituted protein was produced similarly, according to established protocols (Doublie, 1997). TRAPPI subcomplex was purified by Ni-NTA chromatography (Qiagen). Complexes used in guanine nucleotide exchange assays were further purified by gel filtration on a Superdex-200 column (GE Healthcare) to remove the Bet3p/Trs31p heterodimer. The gel filtration buffer (A) contains 10 mM Tris (pH 8.0), 300 mM NaCl, and 1 mM DTT. Complexes used in crystallization were treated with TEV to remove the Trs31p hexahistidine tag.

$His_6$-Ypt1p was also overexpressed in *E. coli* BL21(DE3) cells at 25 °C, as was the selenomethionine substituted Ypt1p, and purified using Ni-NTA resin (Qiagen).

To prepare the $His_6$-Ypt1p/TRAPPI complex for crystallization, a TRAPPI complex consisting of Bet3p, Bet5p, Trs23p, and Trs31p was incubated at room temperature overnight with a molar excess of $His_6$-Ypt1p (residues 1–180) and 20 mM EDTA. EDTA strips magnesium and nucleotides from Ypt1p, thereby facilitating the formation of the Ypt1p/TRAPPI complex. Similar protocols have been used in purifying a number of other GTPase/GEF complexes (see Goldberg, 1998; Renault *et al.*, 2001; or Delprato & Lambright, 2007), and the EDTA treatment does not inactivate Ypt1p (Figure 4A, E, and Esters *et al.*, 2000). The protein mixture was loaded onto a Superdex-200 column (GE Healthcare, in buffer A with 10 mM DTT) to separate the Ypt1p/TRAPPI complex from uncomplexed Ypt1p, excess Bet3p/Trs31p heterodimer, and TEV protease. Ni-NTA resin was used to separate $His_6$-Ypt1p/TRAPPI from TRAPPI. Protein was exchanged into buffer A and concentrated to ~20mg/ml.

### Crystallization

Crystals of the selenomethionine substituted Ypt1p/TRAPPI complex were grown at 22 °C by the hanging-drop vapor diffusion method. Drops consisted of 1.5 μl each of protein solution and reservoir solution (100 mM MES (pH 6.5), 3–5% (w/v) PEG 20,000, 3% (w/v) sorbitol, and 5 mM DTT). Crystals were cross-linked with glutaraldehyde (Heras & Martin, 2005), then transferred through a solution of mother liquor augmented to contain 20% glycerol (v/v), mounted in nylon loops, and flash frozen in liquid nitrogen (Rodgers, 2001). Data were collected at beamline 24-ID-C at the Advanced Photon Source, Argonne National Laboratory, and processed with HKL2000 (Otwinowski & Minor, 1997). Crystals belong to space group

$P2_1$ (a=115.1, b=115.4, c= 290.1 Å, β=90.3°) and diffract to 3.7 Å. They show no evidence of twinning.

### Data Collection and Structure Determination

For phasing, data sets were collected at the selenium edge and at a remote wavelength. To locate the selenium positions we initially worked in a higher symmetry space group, $P4_12_12$, a strategy allowed by pseudosymmetry in the crystal lattice. Once the selenium positions had been located using SHELXD (Schneider & Sheldrick, 2002), we worked in the $P2_1$ space group. One hundred selenium sites were used in calculating phases. The selenium positions were refined, and initial density-modified phases calculated using SHARP (LaFortelle & Bricogne, 1997). There are four copies of each Ypt1p/TRAPPI complex in the asymmetric unit. The four copies were averaged using the RAVE suite of programs (Kleywegt *et al.*, 2001) in conjunction with CCP4 (Collaborative Computational Project, 1994) for improved maps. Electron density maps used for model building were sharpened, with B-factors ranging between −55 and −100 $Å^2$ (Figure S5). In building the model, we were guided by the selenium positions as well as by structures available for vertebrate subunits of TRAPP and for nucleotide bound forms of Ypt1p/Rab1a. Neither the Bet3p C-termini nor the palmitoylate groups in the Bet3p-A channels were modeled initially, and they were added only during refinement. The final model includes residues 6–193 and 8–193 of Bet3p-A and B; 1–21 and 35–156 of Bet5p; 2–55, 67–75, 104–148, and 169–219 of Trs23p; and 55–103 and 165–282 of Trs31p. For Ypt1p, residues 4–31 and 37–174 were modeled.

The initial model was built with O (Kleywegt & Jones, 1997). The structure was refined by iterative cycles of manual refitting, torsion angle dynamics, and B-factor refinement in CNS (Brunger *et al.*, 1998). Phi/psi restraints were placed on helical regions, and the four complexes in the asymmetric unit were restrained to be similar. Composite omit maps were a valuable tool in rebuilding, though high temperatures (4000 K) were necessary during the torsion angle dynamics in order to remove phase bias. One round of averaging was applied to the omit maps, and the averaged map was consulted for rebuilding. The density for the Bet3p C-termini and the Bet3p-B palmitoylate groups is clear in all composite omit maps (see Figure S1). Final refinement statistics are shown in Table S1.

Figures were prepared using the programs Ribbons (Carson, 1997) or Grasp (Nicholls, 1993).

### Transient kinetic analysis

Kinetic analysis of nucleotide binding and dissociation were done following established procedures (Hannemann *et al.*, 2005) and are described in the Supplemental Methods. Briefly, nucleotide binding to Ypt1p was measured from the fluorescence enhancement associated with Forster resonance energy transfer from Ypt1p tryptophan residues to bound mant- (N-methylanthraniloyl-) nucleotide (Invitrogen) after rapid mixing under pseudo-first-order conditions ([nucleotide] ≫ [Ypt1p] or [Ypt1p/TRAPPI]). GDP exchange from Ypt1p is limited by dissociation of bound GDP and was measured by quantitation of tritiated-GDP using a filter-based binding assay (Wang *et al.*, 2000) and/or from the fluorescence of mantGDP.

Nucleotide Exchange Assays and *In Vitro* Binding with TRAPPII are described in the Supplemental Methods.

## Supplementary Material

Refer to Web version on PubMed Central for supplementary material.

**Acknowledgements**

We are grateful to Yunrui Du for her gift of yeast genomic DNA, to Hong Zheng for help in overexpressing and purifying mutant TRAPPI subcomplexes, to Wei Wang for data used to assemble Figure 6A, and to the staff at 24-ID at the Advances Photon Source for help in data collection. We thank P. Novick for discussions regarding this manuscript. This work was supported by grants to KMR from the Mathers Foundation and the NIH (GM080616) and to SF-N from the Howard Hughes Medical Institute. EMDLC is supported by grants from the NIH (GM071688), the NSF (MCB-0546353), and the American Heart Association (0655849T). DWR is supported by grants from the NIH (NS38041, DA02243, RR020171). HFC is supported by NIH predoctoral award 1F31DC009143-01.

## References

Boriack-Sjodin PA, Margarit SM, Bar-Sagi D, Kuriyan J. The structural basis of the activation of Ras by Sos. Nature 1998;394:337–343. [PubMed: 9690470]

Bos JL, Rehmann H, Wittinghofer A. GEFs and GAPs: critical elements in the control of small G proteins. Cell 2007;129:865–877. [PubMed: 17540168]

Brunger AT, et al. Crystallography and NMR system (CNS): a new software suite for macromolecular structure determination. Acta Cryst 1998;D54:904–921.

Cai H, Reinisch K, Novick S. Coats, tethers, Rabs, and SNAREs work together to mediate the intracellular destination of a transport vesicle. Dev Cell 2007a;12:671–82. [PubMed: 17488620]

Cai H, Yu S, Menon S, Cai Y, Lazarova D, Fu C, Reinisch K, Hay JC, Ferro-Novick S. TRAPPI tethers COPII vesicles by binding the coat subunit Sec23. Nature 2007b;445:941–944. [PubMed: 17287728]

Cai H, Zhang Y, Pypaert M, Walker L, Ferro-Novick S. Mutants in *trs120* disrupt traffic from the early endosome to the late Golgi. J Cell Biol 2005;171:823–833. [PubMed: 16314430]

Carson M. Ribbons. Methods in Enzymology 1997;277:493–505. [PubMed: 18488321]

Collaborative Computational Project Number 4. The CCP4 Suite: Programs for Protein Crystallography. Acta Cryst D 1994;50:760–763. [PubMed: 15299374]

Delprato A, Merithew E, Lambright DG. Structure, exchange determinants, and family-wide Rab specificity of the tandem helical bundle and Vps9 domains of Rabex-5. Cell 2004;118:607–617. [PubMed: 15339665]

Delprato A, Lambright DG. Structural basis for Rab GTPase activation by VPS9 domain exchange factors. Nat Struct Mol Biol 2007;14:406–412. [PubMed: 17450153]

Dong G, Medkova M, Novick P, Reinisch KM. A catalytic coiled coil: structural insights into the activation of the Rab GTPase Sec4p by Sec2p. Mol Cell 2007;25:455–62. [PubMed: 17289591]

Doublie S. Preparation of selenomethionyl proteins for phase determination. Methods Enzymol 1997;276:523–530. [PubMed: 9048379]

Eathiraj S, Pan X, Ritacco C, Lambright DG. Structural basis of a family-wide Rab GTPase recognition by rabenosyn-5. Nature 2005;436:415–419. [PubMed: 16034420]

Esters H, Alexandrov K, Iakovenko A, Ivanova T, Thomä N, Rybin V, Zerial M, Scheidig AJ, Goody RS. Vps9, Rabex-5, and DSS4: Proteins with weak but distinct nucleotide-exchange activities for Rab proteins. J Mol Biol 2001;310:141–156. [PubMed: 11419942]

Goldberg J. Structural basis for activation of the ARF GTPase: Mechanisms of guanine nucleotide exchange and GTP-myristoyl switching. Cell 1998;95:237–248. [PubMed: 9790530]

Grosshans BL, Ortiz D, Novick P. Rabs and their effectors: achieving specificity in membrane traffic. Proc Natl Acad Sci U S A 2006;103:11821–7. [PubMed: 16882731]

Hannemann DE, Cao W, Olivares AO, Robblee JP, De La Cruz EM. Magnesium, ADP, and actin binding linkage of myosin V: evidence for multiple myosin V-ADP and actomyosin V-ADP states. Biochem 2005;44:8826–8840. [PubMed: 15952789]

Heras B, Martin JL. Post-crystallization treatments for improving diffraction quality of protein crystals. Acta Crystallogr D 2005;61:1173–80. [PubMed: 16131749]

Itzen A, Rak A, Goody RS. Sec2 is ahighly efficient exchange factor for the Rab protein Sec4. J Mol Biol 2007;365:1359–1367. [PubMed: 17134721]

Jahn R, Scheller RH. SNAREs—engines for membrane fusion. Nat Rev Mol Cell Biol 2006;7:631–643. [PubMed: 16912714]

Jones S, Newman C, Liu F, Segev N. The TRAPP complex is a nucleotide exchanger for Ypt1 and Ypt31/32. Mol Biol Cell 2000;11:4403–4411. [PubMed: 11102533]

Kim MS, Yi MJ, Lee KH, Wagner J, Munger C, Kim YG, Whiteway M, Cygler M, Oh BH, Sacher M. Biochemical and crystallographic studies reveal a specific interaction between TRAPP subunits Trs33p and Bet3p. Traffic 2005a;6:1183–95. [PubMed: 16262728]

Kim YG, Sohn EJ, Seo J, Lee KJ, Lee HS, Hwang I, Whiteway M, Sacher M, Oh BH. Crystal structure of bet3 reveals a novel mechanism for Golgi localization of tethering factor TRAPP. Nat Struct Mol Biol 2005b;12:38–45. [PubMed: 15608655]

Kim YG, Raunser S, Munger C, Wagner J, Song YL, Cygler M, Walz T, Oh BH, Sacher M. The architecture of the multisubunit TRAPP I complex suggests a model for vesicle tethering. Cell 2006;127:817–830. [PubMed: 17110339]

Klebe C, Prinz H, Wittinghofer A, Goody RS. The kinetic mechanism of Ran-nucleotide exchange catalyzed by RCC1. Biochemistry 1995;34:12543–12552. [PubMed: 7548002]

Kleywegt GJ, Brunger AT. Checking your imagination: applications of the free R value. Structure 1996;4:897–904. [PubMed: 8805582]

Kleywegt GJ, Jones TA. Model building and refinement practice. Methods Enzymol 1997;277:208–230. [PubMed: 18488311]

Kleywegt GJ, Zou JY, Kjeldgaard M, Jones TA. International Tables for Crystallography 2001;F:353–356. 366–367.

Koumandou VL, Dacks JB, Coulson RMR, Field MC. Control systems for membrane fusion in the ancestral eukaryote; evolution of tethering complexes and SM proteins. BMC Evolutionary Biol 2007;7:29–46.

Kuehn MJ, Hermann JM, Schekman R. COPPII-cargo interactions direct protein sorting into ER-derived transport vesicles. Nature 1998;391:187–190. [PubMed: 9428766]

Kummel D, Heinemann U, Veit M. Unique self-palmitoylation activity of the transport protein particle component Bet3: a mechanism required for protein stability. Proc Natl Acad Sci U S A 2006;103:12701–6. [PubMed: 16908848]

Kummel D, Muller JJ, Roske Y, Henke N, Heinemann U. Structure of the Bet3-Tpc6B core of TRAPP: two Tpc6 paralogs form trimeric complexes with Bet3 and Mum2. J Mol Biol 2006b;361:22–32. [PubMed: 16828797]

La Fortelle, E de; Bricogne, G. Maximum-likelihood heavy-atom parameter refinement for multiple isomorphous replacement and multiwavelength anomalous diffraction methods. Methods Enzymol 1997;276:472–494.

Longtine MS, McKenzie A 3rd, Demarini DJ, Shah NG, Wach A, Brachat A, Philippsen P, Pringle JR. Additional modules for versatile and economical PCR-based gene deletion and modification in Saccharomyces cerevisiae. Yeast 1998;14:953–961. [PubMed: 9717241]

Morozova N, Liang Y, Tokarev AA, Chen SH, Cox R, Andrejic J, Lipatova Z, Sciorra VA, Emr SD, Segev N. TRAPPII subunits are required for the specificity switch of a Ypt-Rab GEF. Nat Cell Biol 2006;8:1263–1269. [PubMed: 17041589]

Moyer BD, Allan BB, Balch WE. Rab1 interaction with GM130 effector complex regulates COPII vesicle cis-Golgi tethering. Traffic 2001;2:268–276. [PubMed: 11285137]

Nicholls, A. GRASP: graphical representation and analysis of surface properties (computer program). Columbia University; New York: 1993.

Otwinowski Z, Minor W. Processing of x-ray diffraction data collected in oscillation mode. Methods Enzymol 1997;276:307–326.

Renault L, Kuhlmann J, Henkel A, Wittinghofer A. Structural basis for guanine nucleotide exchange on Ran by the Regulator of Chromosome Condensation (RCC1). Cell 2001;105:245–255. [PubMed: 11336674]

Rodgers DW. Cryocrystallography techniques and devices. International Tables for Crystallography F 2001:202–208.

Sacher M, Barrowman J, Schieltz D, Yates JR 3rd, Ferro-Novick S. Identification and characterization of five new subunits of TRAPP. Eur J Cell Biol 2000;79:71–80. [PubMed: 10727015]

Sacher M, Barrowman J, Wang W, Horecka J, Zhang Y, Pypaert M, Ferro- Novick S. TRAPPI implicated in the specificity of tethering in ER-to- Golgi transport. Mol Cell 2001;7:433–442. [PubMed: 11239471]

Sacher M, Jiang Y, Barrowman J, Scarpa A, Burston J, Zhang L, Schieltz D, Yates JR 3rd, Abeliovich H, Ferro-Novick S. TRAPP, a highly conserved novel complex on the cis-Golgi that mediates vesicle docking and fusion. EMBO J 1998;17:2494–503. [PubMed: 9564032]

Sato Y, Fukai S, Ishitani R, Nureki O. Crystal structure of Sec4p.Sec2p complex in the nucleotide exchanging intermediate state. Proc Natl Acad Sci 2007;104:8305–8310. [PubMed: 17488829]

Schneider TR, Sheldrick GM. Substructure solution with SHELXD. Acta Cryst 2002;D58:1772–1779.

Turnbull AP, Kummel D, Prinz B, Holz C, Schultchen J, Lang C, Niesen FH, Hofmann KP, Delbruck H, Behlke J, Muller EC, Jarosch E, Sommer T, Heinemann U. Structure of palmitoylated BET3: insights into TRAPP complex assembly and membrane localization. EMBO J 2005;24:875–84. [PubMed: 15692564]

Wang W, Sacher M, Ferro-Novick S. TRAPP stimulates guanine nucleotide exchange on Ypt1p. J Cell Biol 2000;151:289–96. [PubMed: 11038176]

Yu S, Satoh A, Pypaert M, Mullen K, Hay JC, Ferro-Novick S. mBet3p is required for homotypic COPII vesicle tethering in mammalian cells. J Cell Biol 2006;174:359–68. [PubMed: 16880271]

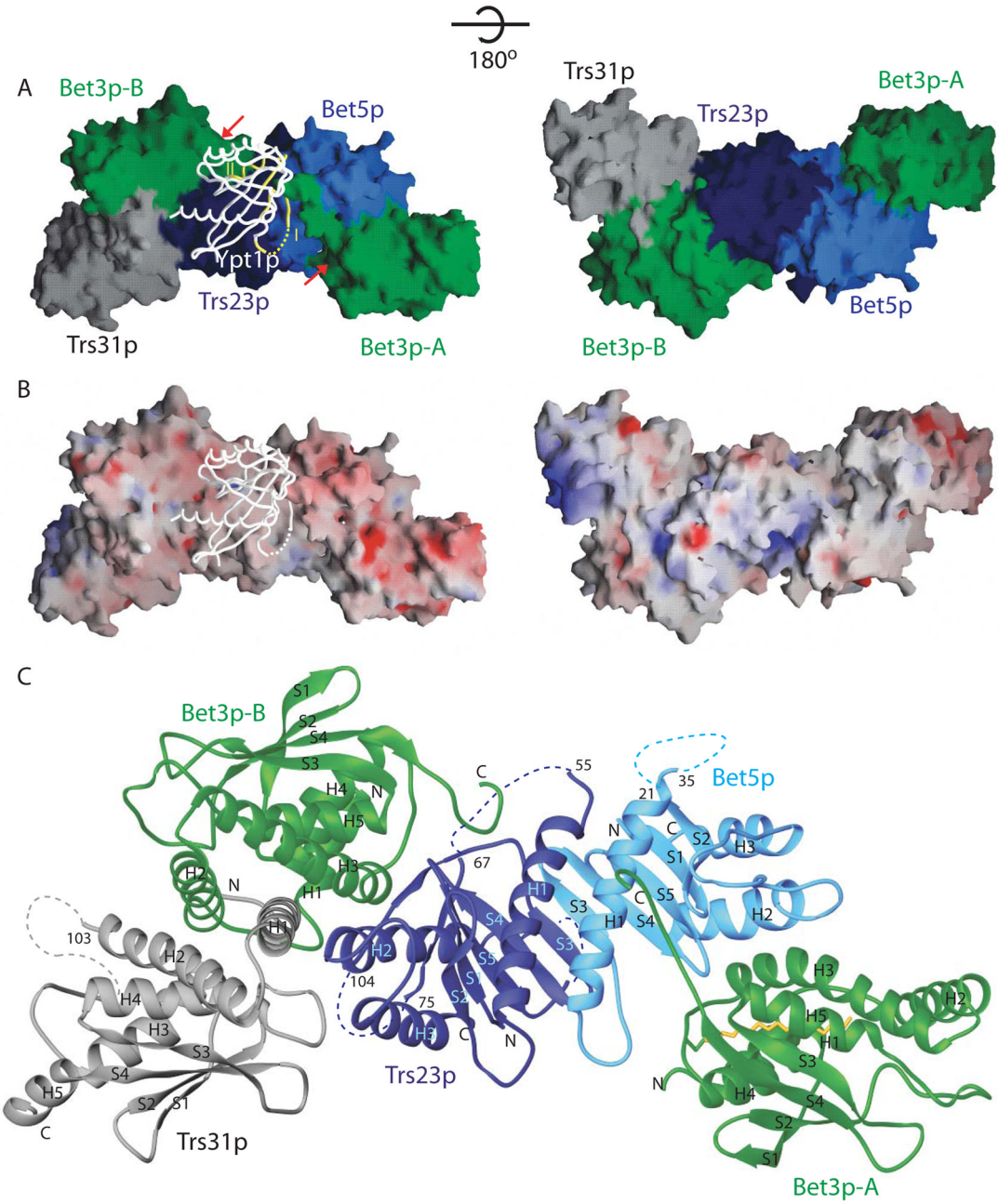


**Figure 1.**

Structure of Ypt1p bound to TRAPPI subcomplex. (A) The TRAPPI complex is shown as a surface representation, and Ypt1p is shown as a backbone worm. In TRAPPI, different polypeptide chains are colored differently. In Ypt1p, switch regions I and II are yellow. At left, the positions of Cys80 and the hydrophobic channels in the two copies of Bet3p are labeled with red arrows. The right panel shows the same complex rotated about the horizontal axis indicated. (B) A surface representation of TRAPPI colored by electrostatic potential (blue=basic; red=acidic), with Ypt1p shown as a backbone worm. The orientations of the protein complexes are identical in panels A and B. (C) A ribbons representation of TRAPPI oriented as in panel A, left. The palmitoylate group modeled into the Bet3p-A hydrophobic channel is yellow.

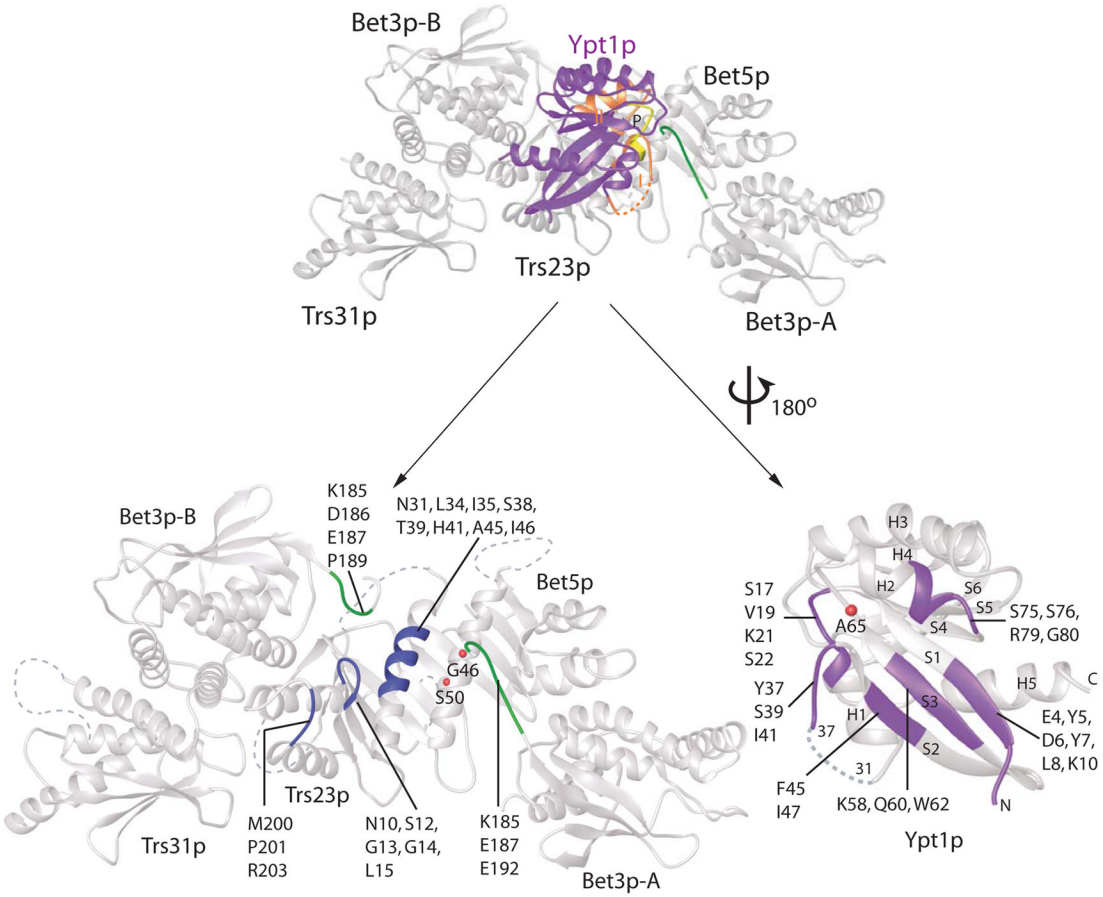


**Figure 2.**

The Ypt1p/TRAPPI interface. At top, the complex is shown with Ypt1p in purple, except for switches I and II (orange) and the P-loop (yellow). The TRAPPI complex is white, except for the C-terminus of Bet3p-A (green). At bottom, Ypt1p has been pulled away from the TRAPPI surface and rotated by 180 ° about a vertical axis. Cα positions of residues within 4 Å of the interface are labeled and colored.

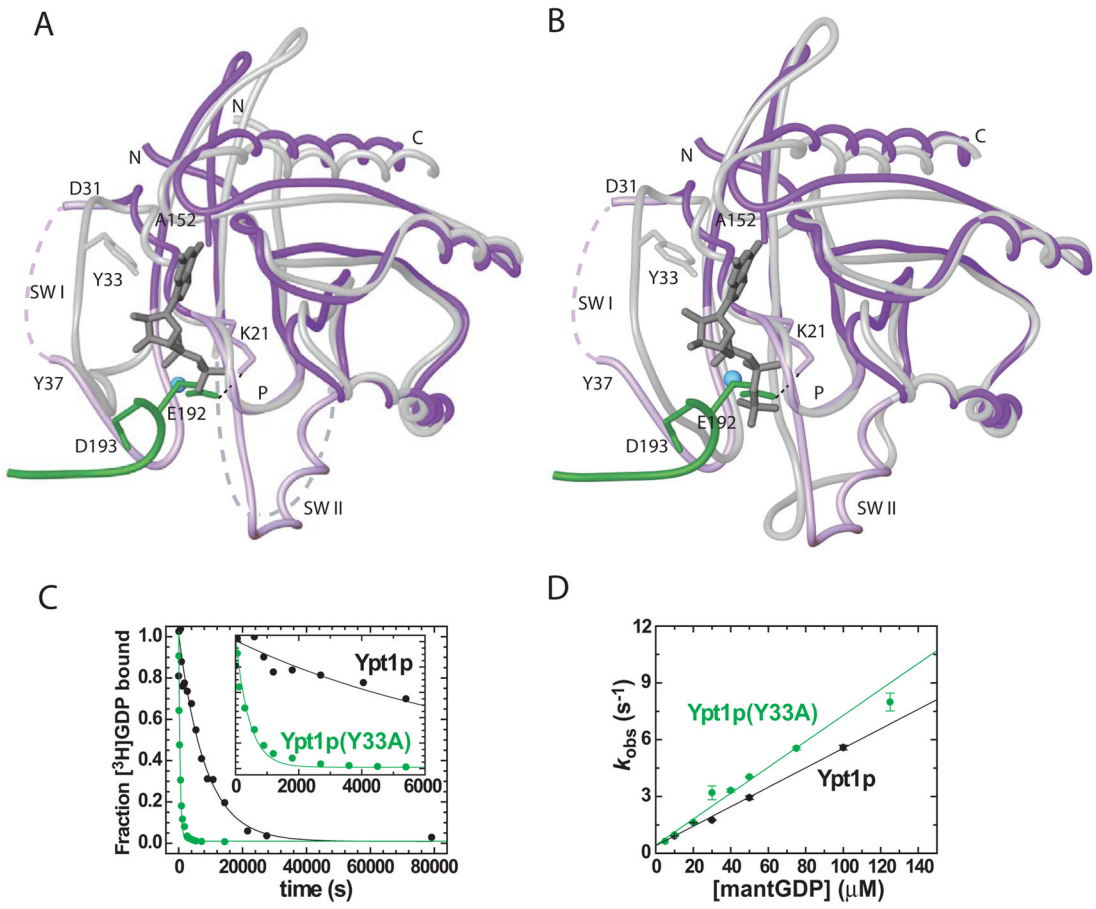


**Figure 3.**

The mechanism for nucleotide exchange. Comparison of the nucleotide-free form of Ypt1p in the Ypt1p/TRAPPI complex with (A) GDP-bound Rab1a (PDB ID 2FOL) and (B) GppNHp-bound Ypt1p (1YZN). The nucleotide-free form of Ypt1p is purple, except for the switch regions and the P-loop (lavender). The C-terminus of Bet3p-A, including the E192 and D193 side chains, is green. Nucleotide-bound forms of Ypt1p/Rab1a are white, including the Y33 side chain. Nucleotide is grey and the magnesium cation blue. (C) GDP dissociates from the Ypt1p (Y33A) mutant ~10 times faster than from wt Ypt1p. Time course of [$^3$H]-GDP dissociation from 400 nM Ypt1p (black) and Ypt1p(Y33A) (green) is shown; it was measured by a filter binding assay described in the Supplemental Methods. Solid line through the data is the best fit to a single exponential yielding the GDP dissociation rate constant ($k_{-GDP}$) of 1.21±0.22 ×10$^{-}$4 s$^{-1}$ for Ypt1p and 16.3±0.6 ×10$^{-4}$ for Ypt1p(Y33A). The inset shows the same data over a shorter time interval. (D) GDP associates with Ypt1p and Ypt1p(Y33A) at similar rates. MantGDP binding to nucleotide-free Ypt1p or Ypt1p(Y33A) was continuously monitored by fluorescence (Figure S6A). The concentration dependence of $k_{obs}$ for Ypt1p (black) and Ypt1p(Y33A) (green) is shown. The second-order association rate constant for GDP binding ($k_{+GDP}$) determined from the slopes of the best fits to the data over this range are 0.05±0.01 μM$^{-1}$ s$^{-1}$ for Ypt1p and 0.07±0.01 μM$^{-1}$ s$^{-1}$ for Ypt1p(Y33A).

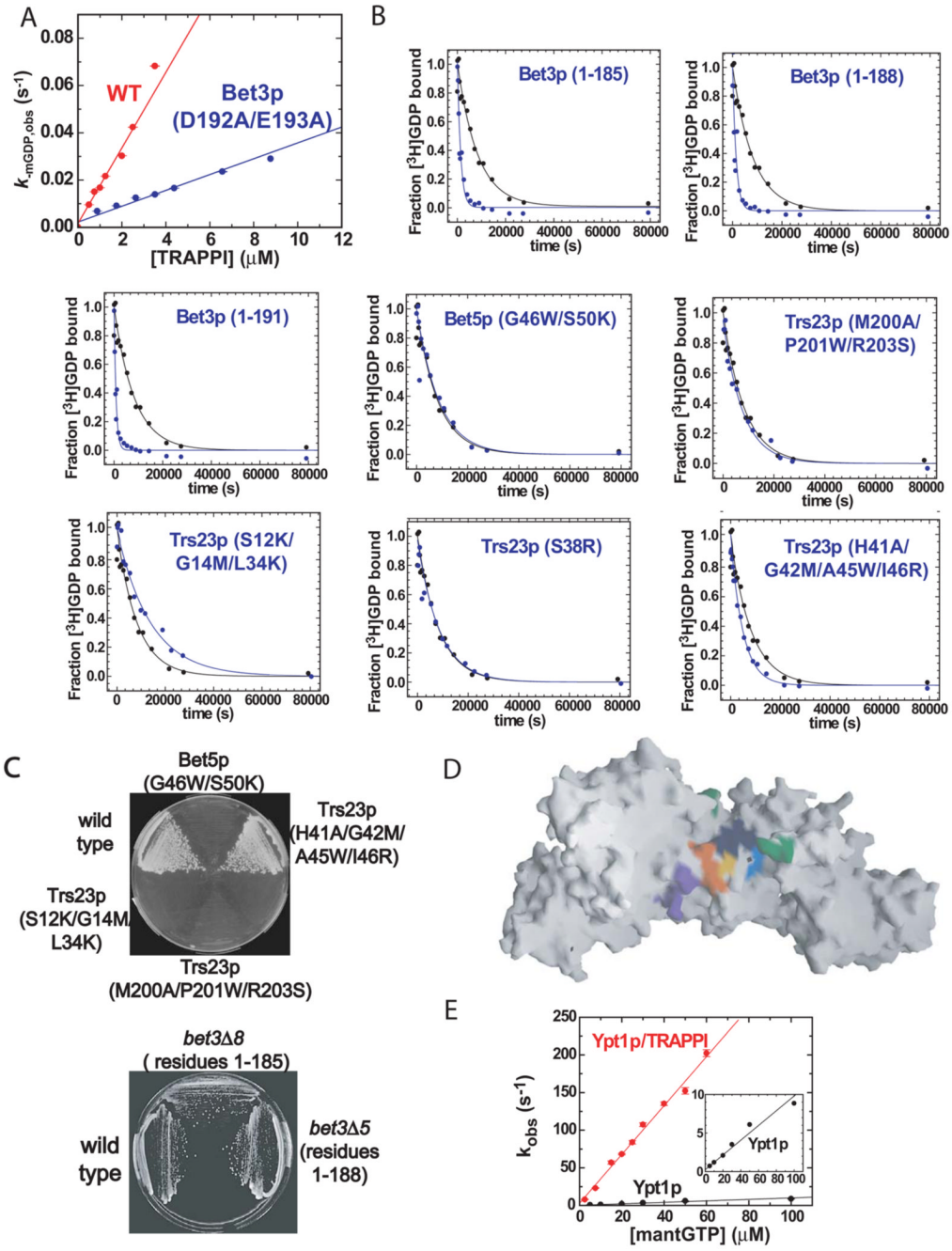


**Figure 4.**

Kinetic and mutational analysis of TRAPPI. Data in (A–B) were used in calculating "$k_{cat}/K_M$" and $k_{-GDP,obs}$ values reported in Table 1. (A) MantGDP dissociation from Ypt1p (250 nM) in the presence of TRAPPI (Bet3p, Bet5p, Trs20p, Trs23p, and Trs31p) and TRAPPI mutants was continuously monitored by fluorescence ($\lambda_{ex}$=280 nm, $\lambda_{em}$=435 nm; Figure S6C). TRAPPI (red) and Bet3p (E192A/D193A) mutant (blue) concentration dependence of the observed GDP dissociation rate constant ($k_{-mGDP,obs}$) is shown; filter binding assays are described in the Supplemental Methods. The solid lines are best fits of the data to linear functions, yielding the catalytic efficiencies (apparent $k_{cat}/K_M$) from the slopes. (B) Other mutants had only residual GEF activities. Time courses of [$^3$H]-GDP dissociation from 400

nM Ypt1p in the absence (black) or presence (blue) of the indicated TRAPPI mutant are shown; Table 1 lists TRAPPI concentrations. Solid lines are the best fits to single exponentials yielding the observed GDP dissociation rate constant ($k_{-GDP,obs}$). (C) Yeast cells harboring point mutations in *bet5* and *trs23*, which reduce GEF activity in vitro, were grown at 25°C on 5-FOA plates. All these mutants were inviable, except for *trs23* (H41A/G42M/A45W/I46R), which also grows at 37°C (data not shown). Yeast cells harboring C-terminal truncations in *bet3*, which reduce GEF activity *in vitro*, were grown at 25 °C and 37 °C on YPD plates. The 37 °C plate is shown. The *bet3* truncation mutants were viable. (D) TRAPPI oriented as in Figure 1A, left. Residues that were mutated are indicated. Green: residues 192–193 in Bet3p. Cyan: 46, 50 in Bet5p; Orange: 12, 14, 34 in Trs23p; Purple: 200–201, 203 in Trs23p.Yellow: 38 in Trs23p. Indigo:41–42, 45–46 in Trs23p. (E) TRAPPI-bound Ypt1p associates with GTP ~30 times faster than Ypt1p alone. MantGTP binding to nucleotide-free Ypt1p or Ypt1p/TRAPPI complex was monitored by fluorescence (Figure S6B). MantGTP concentration dependence of $k_{obs}$ for Ypt1p (black) and Ypt1p/TRAPPI complex (red) is shown. The second-order association rate constant for mantGTP binding ($k_{+GTP}$) determined from the slopes of the best fits of the data are 0.10±0.01 $\mu M^{-}1\ s^{-1}$ for Ypt1p and 3.2±0.1 $\mu M^{-1}\ s^{-1}$ for Ypt1p/TRAPPI.

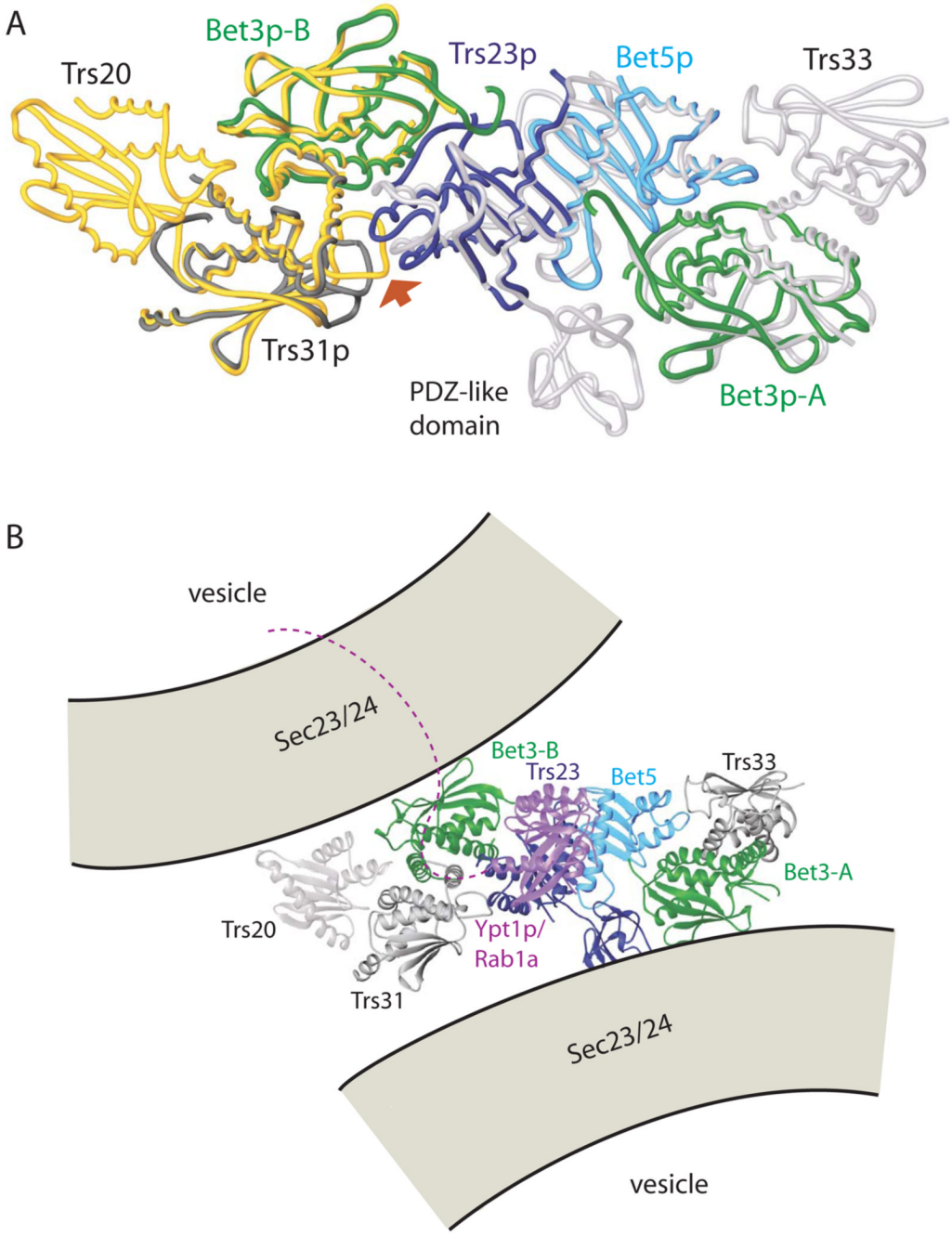


**Figure 5.**

A superposition of the yeast TRAPPI subcomplex containing Trs31p/Bet3p-B/Trs23p/Bet5p/Bet3p-A with the Trs20/Trs31/Bet3-B (yellow, PDB ID 2J3W) and Trs23/Bet5/Bet3-A/Trs33 (white, 2J32) complexes from vertebrates. A PDZ-like domain is present only in mammalian Trs23. Yeast proteins are colored as in Figure 1, (A) and (C), and the complex is oriented as in panels A–C, left. The largest deviations between the yeast and vertebrate assemblies are at the 3-way interface between Trs23p, Trs31p, and Bet3p-B (arrow). (B) Model for the mammalian TRAPP core as it tethers two COPII coated vesicles *via* interactions between Bet3 subunits of TRAPP and Sec23 of the COPII coat. The two copies of Bet3 and the two vesicles are related by the same 2-fold rotation about an axis perpendicular to the plane of the page.

Equivalent surface patches on Bet3-A and –B are accessible to both vesicles only if TRAPP is oriented as shown. The C-terminal residues (175–206) absent from Ypt1p (purple) in our structure could span the ~40 Å to the membrane. Ypt1p/Rab1a becomes anchored in the membrane by its prenylated C-terminus.

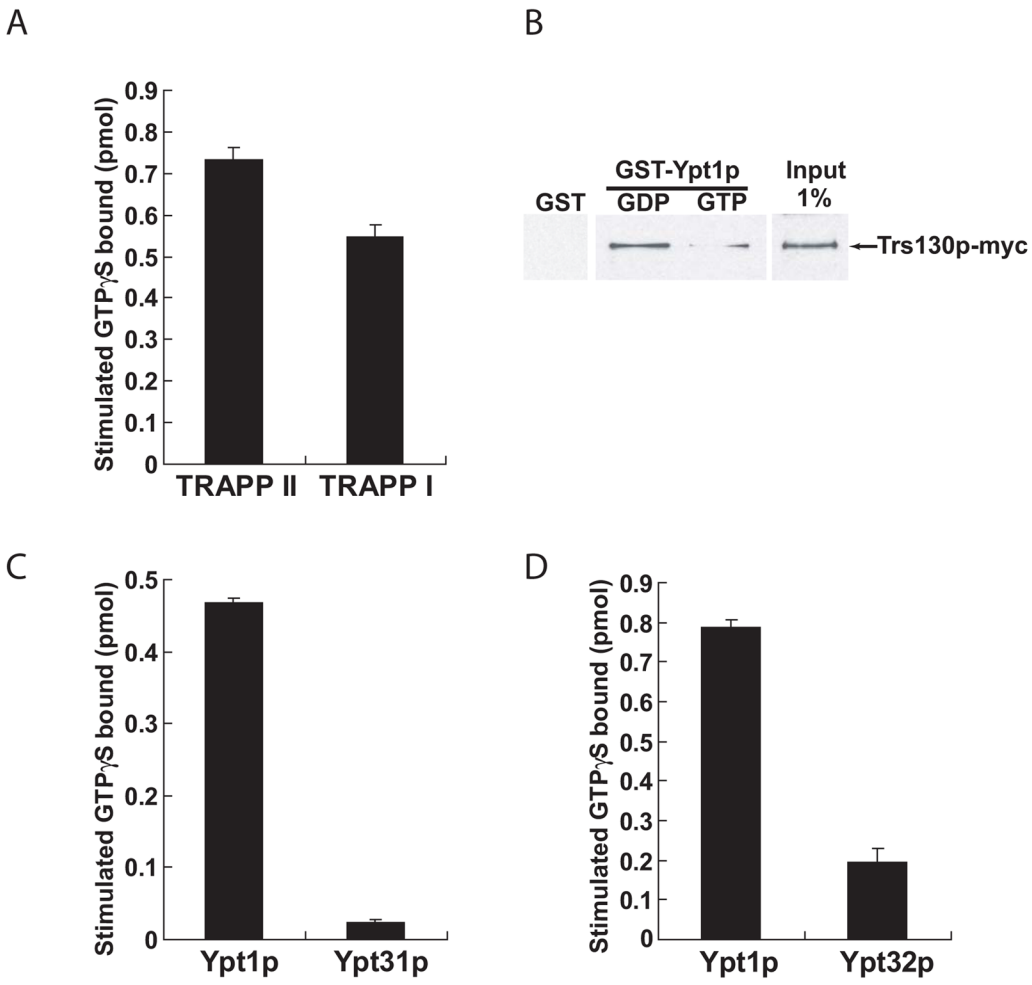


**Figure 6.**

Yeast TRAPPII potently stimulates the GEF activity of Ypt1p, but not Ypt31p or Ypt32p. (A) Protein A tagged TRAPPI and TRAPPII were prepared as described in Supplemental Methods. The GEF activity on Ypt1p, stimulated by TRAPPI and TRAPPII, was normalized to Trs33p. The assay is described in the Supplemental Methods. The data shown were obtained from four separate experiments. Error bars are SEM. (B) Equivalent amounts of recombinant GST, GST-Ypt1p-GDP and GST-Ypt1p-GTP were loaded with nucleotide as described in Supplemental Methods, incubated with yeast lysate as before (Wang *et al*., 2000), and blotted for the TRAPPII-specific subunit Trs130p. (C) The TRAPPII complex, isolated as described above, was assayed for its ability to stimulate nucleotide exchange on Ypt31p and (D) Ypt32p. For comparison, an equivalent amount of TRAPPII was assayed for its ability to activate Ypt1p. The amount of TRAPPII assayed in (C) and (D) was not equivalent. Error bars are SEM.

**Table 1**

Activation of Ypt1p by TRAPPI and TRAPPI mutants

| Construct | color in Figure 4D | [TRAPPI] (μM) | $k_{-GDP,obs}$($s^{-1}$)[1] | Relative rate increase[2] | "$k_{cat}/K_M$"[3] ($\mu M^{-1}$ $s^{-1}$) | Growth Phenotype[4] |
|---|---|---|---|---|---|---|
| no TRAPPI | | 0 | $1.21 \times 10^{-4} \pm 0.22 \times 10^{-4}$ | 1 | N. A. | N. A. |
| TRAPPI, wt | | 3.5 | >0.07 | >400 | 0.016 ± 0.001 | + |
| TRAPPI Bet3p (E192A/D193A) | Green | 10 | >0.03 | >400 | 0.003 ± 0.001 | N.A. |
| TRAPPI Bet3p truncation (1–185 only) | | 18 | $7.43 \times 10^{-4} \pm 0.98 \times 10^{-4}$ | 6 | < 0.0001 | + |
| TRAPPI Bet3p truncation (1–188 only) | | 24 | $7.03 \times 10^{-4} \pm 1.93 \times 10^{-4}$ | 6 | < 0.0001 | + |
| TRAPPI Bet3p truncation (1–191 only) | | 15 | $1.22 \times 10^{-3} \pm 0.19 \times 10^{-4}$ | 10 | < 0.0001 | N.A. |
| TRAPPI Bet5p (G46W/S50K) | Cyan | 28 | $1.14 \times 10^{-4} \pm 0.33 \times 10^{-4}$ | 1 | < 0.0001 | - |
| TRAPPI Trs23p (H41A/G42M/A45W/ I46R) | Indigo | 30 | $2.03 \times 10^{-4} \pm 0.29 \times 10^{-4}$ | 2 | < 0.0001 | + |
| TRAPPI Trs23p (M200A/P201W/ R203S) | purple | 26 | $1.30 \times 10^{-4} \pm 0.24 \times 10^{-4}$ | 1 | < 0.0001 | - |
| TRAPPI Trs23p (S38R) | Yellow | 35 | $1.16 \times 10^{-4} \pm 0.084 \times 10^{-4}$ | 1 | < 0.0001 | - |
| TRAPPI Trs23p (S12K/G14M/L34K) | orange | 28 | $7.2 \times 10^{-5} \pm 9.6 \times 10^{-6}$ | 1 | < 0.0001 | - |

[1] observed GDP dissociation rate constant

[2] Relative to Ypt1p in the absence of TRAPPI

[3] Catalytic efficiency, taken as initial slope of TRAPPI concentration dependence on exchange rate $k_{-GDP,obs}$ at subsaturating TRAPPI concentration (see Delprato *et al*., 2004).

[4] +/− indicates viability/inviability; "N.A." means "not available/applicable".